THE SIMULATION OF PREARCING CHARACTERISTICS OF FUSE ELEMENTS IN THE FINITE ELEMENT METHOD

Meng Xian-zhong   Wang Ji-mei

Xi'an Jiaotong University
The People's Republic of China

Abstract

The authors use the finite element method to calculate the prearcing characteristics, theoretically explain the calculation results, compare the virtual t-I characteristic and the theoretical t-I characteristic consider the deviation very small and the method can be used in the fuse-element design.

1. INTRODUCTION

A lot of different methods have been developed for the simulation of prearcing characteristics of notched fuse elements with heavy short circuit currents, as is well known, the simulation is very sucessful, for example, the finite difference method (1). If the distributions of temperature and electric potential are taken into acount for different shapes of notched fuse-elements, the finite element method would be more convenient because of its process of boundary conditions, fuse-element geometry and the positive stiffness matrix, that is why the f.e.m. (finite element method) is used here. After the distributions are carried out, all the parameters required can be obtained to simulate the prearcing phenomena.

2. THEORETICAL ANALYSIS

2.1 General discription

As far as two dimensional electric current flow fields and temperature fields, general equations are:

$$\frac{\partial}{\partial x}\left(K_x\frac{\partial \phi}{\partial x}\right) + \frac{\partial}{\partial y}\left(K_y\frac{\partial \phi}{\partial y}\right) = f(x,y) + K_t.\dot{\phi}_t \qquad (1)$$

$$\forall\ (x,y) \in \Omega$$

where K_x, K_y, K —— conduction coefficient, K_t —— damped coefficient, ϕ —— potential function, $\dot{\phi}$ —— derivative of potential function, Ω —— calculation region.

boundary conditions:

$$\phi = \phi(x,y,t) \qquad t > 0, \quad \text{on} \quad \Gamma_1$$

$$K_x\frac{\partial \phi}{\partial x}n_x + K_y\frac{\partial \phi}{\partial y}n_y + q(x,y,t) = 0 \qquad t > 0, \quad \text{on} \quad \Gamma_2$$

$$\Gamma = \Gamma_1 \cup \Gamma_2 \qquad (2)$$

initial conditions:

$$\phi = \phi_0(x,y) \quad t = 0, \quad \forall(x,y) \in \Omega \quad \dot{\phi} = \xi_0(x,y) \quad t = 0, \quad \forall(x,y) \in \Omega \qquad (3)$$

By using the f.e.m. (2), the following equations can stem from (1),(2),(3).

$$\left[K_t\right]^{(e)}\left\{\dot{\phi}\right\}^{(e)} + \left[K\right]^{(e)}\left\{\phi\right\}^{(e)} + \left\{R_1(t)\right\}^{(e)} = \left\{0\right\}^{(e)}$$

Where

$$K_{tij} = \int_{\Omega^{(e)}} K_t \cdot N_i \cdot N_j \, d\Omega^{(e)}; \quad K_{ij} = \int_{\Omega^{(e)}} \left(K_x \cdot \frac{\partial N_i}{\partial x} \cdot \frac{\partial N_j}{\partial y} + K_y \frac{\partial N_i}{\partial y} \cdot \frac{\partial N_j}{\partial y}\right) \cdot d\Omega^{(e)}$$

$$R_{1i} = \int_{\Omega^{(e)}} f \cdot N_i \cdot d\Omega^{(e)} + \int_{\Gamma_2^{(e)}} q_i \cdot d\Gamma_2^{(e)}$$

The resultant equation is

$$[C]\cdot\{\dot{\phi}\} + [K]\cdot\{\phi\} = \{R(t)\} \qquad (4)$$

Where $[C]$ —— Thermal capacity matrix (or damped matrix);
$[K]$ —— Stiffness matrix; $[R(t)]$ —— Right hand vector.

Supposing that $t_\theta = t_n + \theta \cdot \Delta t$, $\quad \{\dot{\phi}\}_\theta = (\{\phi\}_{n+1} - \{\phi\}_n)/\Delta t$;

$$\{R(t_\theta)\} = (1-\theta)\{R(t)\}_n + \theta\{R(t)\}_{n+1} \ ; \qquad \{\phi\}_\theta = (1-\theta)\{\phi\}_n + \theta\{\phi\}_{n+1}$$

According to (4) we get

$$[C]\cdot\{\dot{\phi}\}_\theta + [K]\{\phi\}_\theta = \{R(t_\theta)\} \ (5) \ \text{and} \quad [\bar{K}]\{\phi\}_{n+1} = [\bar{R}]_{n+1} \qquad (6)$$

where $[\bar{K}] = \theta[K] + 1/\Delta t\cdot[C]$; $[\bar{R}]_{n+1} = \{-(1-\theta)[K] + 1/\Delta t\cdot[C]\}\cdot\{\phi\}_n + (1-\theta)\cdot\{R\}_n + \theta\{R\}_{n+1}$.
$\{\phi\}_{n+1}$ is unknown array and other parameters are known , so the equation (6) is solvable.

2.2 The electric current flow field
When electric currents flow through the fuse-element, the electric potential equation is stated as follows:

$$\frac{\partial}{\partial x}(\gamma\frac{\partial\phi}{\partial x}) + \frac{\partial}{\partial y}(\gamma\frac{\partial\phi}{\partial y}) = 0$$

Because of the symmetry of the fuse-element as shown in Fig. 1 (A), the calculation region may be greatly simplified into Fig. 1 (B) and the current direction is taken as that of X-axis.

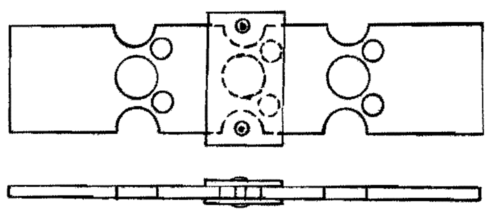

Fig. 1 (A) Fuse-element

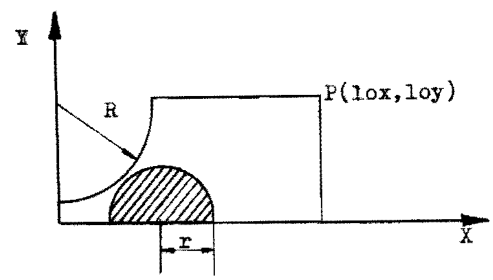

Fig. 1 (B) Calculation region

Considering the geometry of the fuse-element, Lox > R, Lox > r, in order to decrease the calculation time, supposing

$$\phi\Big|_{x=0} = 0, \quad \gamma\frac{\partial\phi}{\partial x}\Big|_{x=lox} = J_0$$

where J_0 is a constant determined by the transient current through the fuse-element.
$\gamma\frac{\partial\phi}{\partial n} = 0$ on the other boundaries therefore the electric potential distribution satisfies the following equation:

$$\frac{\partial}{\partial x}(\gamma\frac{\partial\phi}{\partial x}) + \frac{\partial}{\partial y}(r\frac{\partial\phi}{\partial y}) = 0, \quad \phi\Big|_{x=0} = 0, \quad \gamma\frac{\partial\phi}{\partial x}\Big|_{x=lox} = J_0 \tag{7}$$

It is the special form of (1),(2),(3), after solving $\{\phi\}$, the electric strenth and the current density distribution can be gotten from $E_x = -\partial\phi/\partial x$, $E_y = -\partial\phi/\partial y$, $J_x = \gamma E_x$, $J_y = \gamma E_y$. For the simplicity, is taken as only a function of the position or the local temperature, during the melting of the fuse-element, the resistance coefficient is greatly changable, it is therefore not suitable that γ is considered not to vary with the time variable, at least, it would lead to a large model error. The heat energy produced by the current heating effect in dv at any point p(x,y) in the unit time and volume is

$$Q(IE) = \gamma E_x^2 + \gamma E_y^2 \tag{8}$$

2.3 The temperature field of the fuse-element
The heat conduction equation (2), (3) is

$$\rho C\frac{\partial T}{\partial t} = \frac{\partial}{\partial x}(K_x\frac{\partial T}{\partial x}) + \frac{\partial}{\partial y}(K_y\frac{\partial T}{\partial y}) + \frac{\partial}{\partial Z}(K_z\frac{\partial T}{\partial z}) + q'(x,y,z,t) \tag{9}$$

it is difficult to precisely and directly calculate the temperature distribution of the fuse-element and its temperature field in the media (fillers), because the caps, tags and fillers surrounding the fuse-element and the surrounding temperature in the media influence on thermal fields, especially the precise thermal data of fuse fillers are lack.
In addition, there are some more problems in the calculation of long time transient fields which need to be solved, for example, the stability of solution, the velocity of convergence and the cost of calculation (cpu time), what is more, the coupled two dimensional problems with the electric field.
We start with the penetration depth to discuss how to simplify equation (9). The penetration depth of thermal fields:

$$\delta(t) = \sqrt{12\alpha_0 t}, \quad \alpha_0 = K/\rho C \tag{10}$$

where t is time variable for copper, silver, quartz and PTFE, we can get the following results:

$$\alpha_{o\,Cu}/\alpha_{oq} = 419.036, \quad \delta_{Cu}/\delta_q = 20.47; \quad \alpha_{o\,Ag}/\alpha_{oq} = 625.62, \quad \delta_{Ag}/\delta_q = 25.012$$

$$\alpha_{oF}/\alpha_{oq} = 2.38365 - 0.76778; \quad \delta_q/\delta_F = 2.6055 - 1.30245$$

A. It is obvious that for small time or short circuit current, comparing δ_{cu}, δ_{Ag} with δ_q neglecting δ_q can't cause large error, the range of time depends on the fuse geometry and the calculation accuracy required. In other words, within this range, three dimensional heat conduction equation can be deduce to two dimensional heat conduction equation.

B. For medium and long time overload, we take the surfacial dissipated coefficient into acount which can be obtained from the experimental results, this item is apt to take part in the f.e.m. equations.

Another method for long time overload is to use semi-experienced formula which is based on the f.e.m. and the heat conduction theory.
In case B, we must describe the item $-\int_{\Omega^{(e)}} \mu \cdot N_i d\Omega^{(e)}$ and put it into R_{1i}. Up to now, we can get the following equations;

$$\rho C\frac{\partial T}{\partial t} = \frac{\partial}{\partial x}(K_x\frac{\partial T}{\partial x}) + \frac{\partial}{\partial Y}(K_y\frac{\partial T}{\partial y}) + q'(x.y.t)$$

$$K\frac{\partial T}{\partial n}(x,y,t) = q_B \;; \qquad T(x,y,0) = C_0 \qquad (11)$$

The general calculation region is shown in Fig. 1 (B). We don't consider the conduction among the symetric sections of fuse elements. With short circuit current, $q_B = 0$, that means the heat conduction doesn't exist in the element symetric lines and on the contact surfaces between fillers and the fuse-element or covered materials, if any, and the fuse element. In general, q_B depends on the surfacial state of heat discipation and $q_B \neq 0$ (related to μ), C_0 indicates the initial temperature distribution and takes a constant. We also give K_x, K_y, ρ, C constant values respectively before the fuse-element melts.

3. PHASE CHANGE ALGORITHMS

When electric currents flow through the fuse-element, the element and the media around are heated due to Joule effect, and the temperature rises, if the energy put into the element is more than that discipated, the element temperature will go high, while the temperature is up to or above the melting point of the fuse-element, the solid-liquid phase change occurs, if it continues, maybe the liquid-gas phase change will take place.
As a basic element, the triangle element is used here, the average temperature of the local element or division element:

$$T_{ave.} = 1/3\sum_{i=1}^{3} T_i, \qquad \Delta T_m = H_m/C_{ps} \qquad (12)$$

for each triangle element, when T_{ave} exceeds T_m, it should be changed to T_m, and write down $(T-T_m)$ or (T_i-T_m). If $(T-T_m) \geqslant \Delta T_m$, the temperature of local element is admitted to increase in normal way, for each node, it is similar. Further more, the similar algorithm is suitable for the vaporization and M-spots.
It is hard to say when notched elements begin to arc, because the initial arc is related to the electric current density, the fuse-element geometry, the properties of materials and so on. We suppose that arc occurs when the temperature of local element begins to rise after the melting of the local region, therefore the temperature lies in the range of T_m to T_a or more high.

The prearcing virtual time $\quad t_v = \int i^2 dt \,/\, I_p^2 \qquad (13)$

The calculation results prove that it is true.

4. PROGRAM DESIGN

The diagram (see Fig. 2) shows us how to finish the simulation work in f.e.m. Fig.2(B) gives the block for CURRENT DISTRIBUTION AND TEMPERATURE DISTRIBUTION. All the programs are written in FORTRAN 77 running well in Dps 8/52 in COMPUTER CENTER of Xi'an Jiaotong University, China.

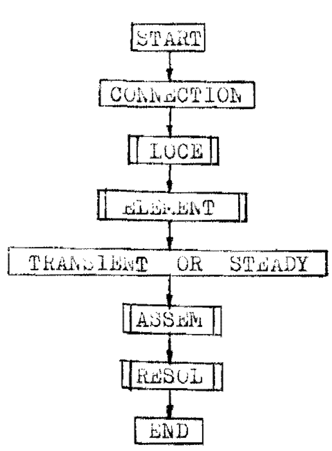

FIG. 2 (B) BLOCK DIAGRAM

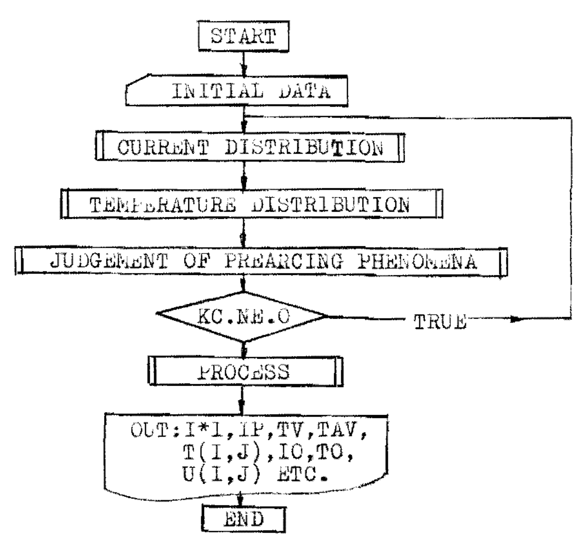

FIG. 2 (A) BLOCK DIAGRAM

5. THE FORMULA FOR LOW OVERLOAD

We recommand a simi-experienced formula which is suitable for the fuse-element with M-spots and covered materials throughlow overload currents.
The virtual time $t_v = t_m + t_r$, where t_r depends on the following equations:

$$\vartheta = \frac{I^2}{I_c^2}\cdot T_w(1-e^{-t_r/\tau}); \quad \tau = \rho C T_w / C_e . I_c^2 \cdot \rho_0(1-\eta) \;; \quad T_w = K_0(T_{sold} + H_m/C_{pl}) \qquad (14)$$

where C is specific heat, C_e is f.e.m. division coefficient, η is heat discipated coefficient from the specified elements and τ is time constant, $0 \leqslant K_0 \leqslant 1$.

The M-effect time $t_m = Z^2/N_p \cdot D$ (15)

where N_p is the distribution coefficient, Z is the element thickness and D is the diffusion coefficient. If $\nu = (T_{sold} + H_m/C_{pl})$, it is said that the melted M-spots will flow along the element to the neck and cause the rupture of the fuse element due to M-effect.

6. APPLICATIONS

The programs in f.e.m. and the formula (14), (15) have been used to simulate the prearcing phenomena of a type of full range fuses and got some sucessful results given in figures (from Fig. 3 to Fig. 10), the element of which is shown in Fig. 1 (A). The fuse rated current and voltage are respectively 63A and 500V. For different shapes of elements, the parameters needed to be changed are the f.e.m. division grid and physical data of the fuse-element, so it is very convinient for users and designers to use this method to simulate.

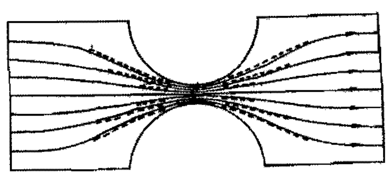

Fig. 3 Current flow distribution

——— Distribution in cold state

----- Distribution in hot state

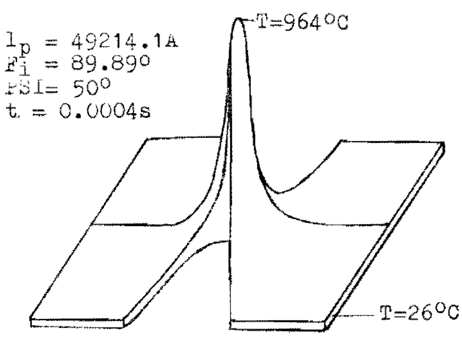

Fig. 4 Temperature field with short circuit current

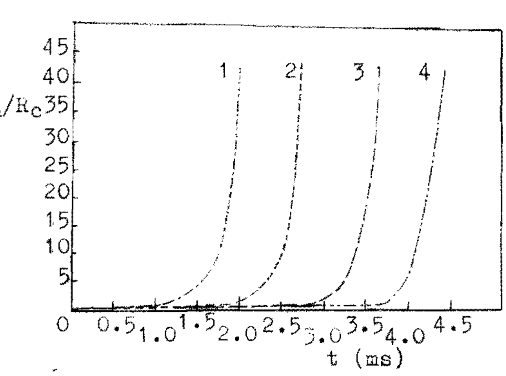

Fig. 5 Hot state R_h/Cold state R_c VS time

Curve 1 I_p = 5001.33A, φ = 88.78°, ψ = 67°

Curve 2 I_p = 3889.69A, φ = 88.79°, ψ = 60°

Curve 3 I_p = 2500,67A, φ = 88.96°, ψ = 47°

Curve 4 I_p = 1750.57A, φ = 89.16°, ψ = 47°

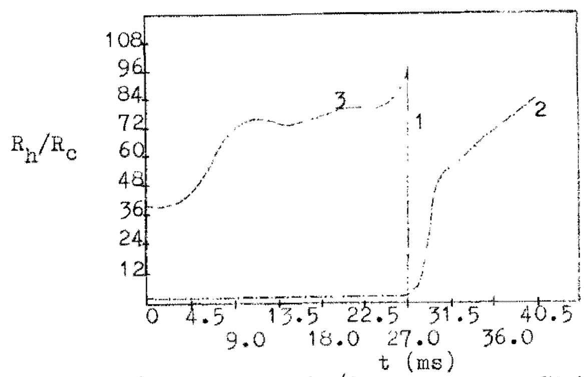

Fig. 6 Hot state R_h/Cold state R_c VS time
I_p = 580.32A, φ = 83.94°, ψ = 56°

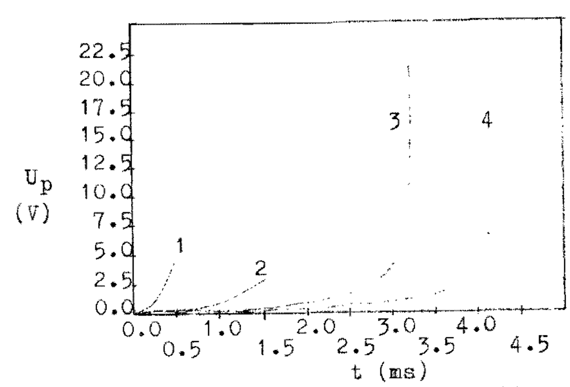

Fig. 7 Prearcing voltage VS time

Curve 1 I_p = 50021.5A, φ =89.89°, ψ = 67°

Curve 2 I_p = 8753.50A, φ =89.91°, ψ = 60°

Curve 3 I_p = 3070.92A, φ =88.82°, ψ = 40°

Curve 4 I_p = 1750.57A, φ =89.16°, ψ = 47°

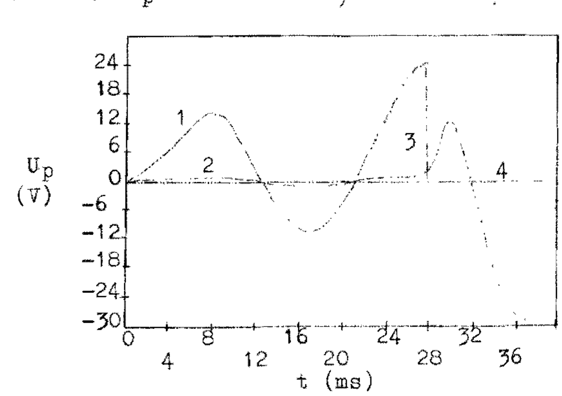

Fig. 8 Prearcing voltage VS Time
I_p = 580.32A, φ = 83.94°, ψ = 56°

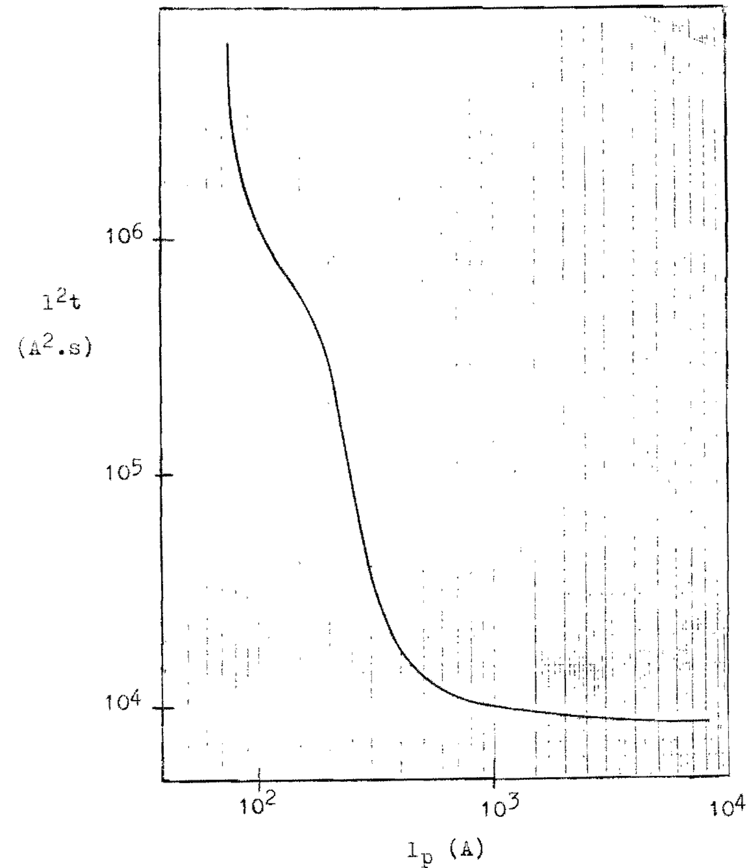

Fig. 9 I^2t - I_p characteristic

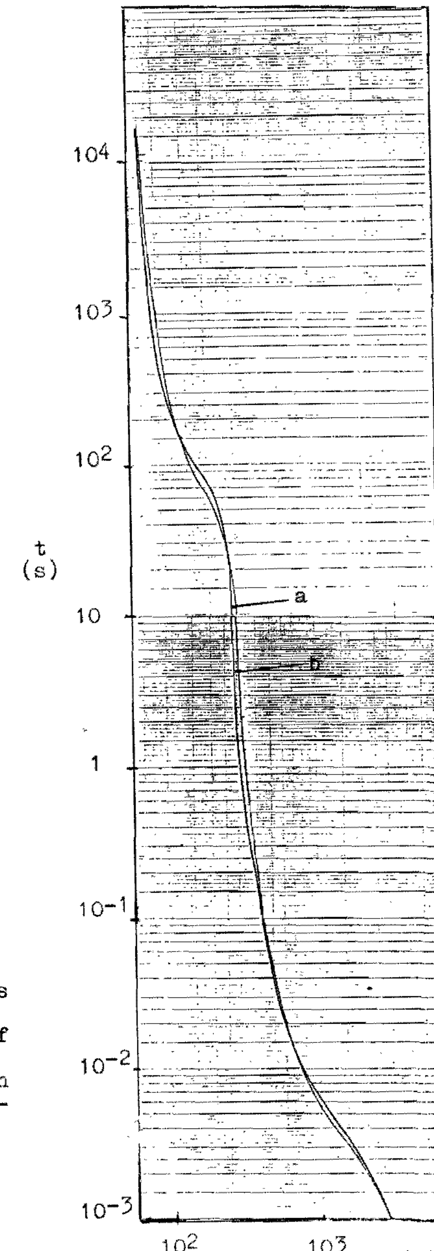

a. theoretical curve

b. test results

Fig.10 t—I characteristic

7. DISCUSSION

Fig. 2 is suitable for current fields and temperature fields of the fuse-element on principle, in oder to reduce the CPU time, small time steps Δt are taken to solve the two set of equations respectively for compensation.
It will be seen from Fig. 3 that the current flowing through element is concentrated towards the edge with time, especially in the constrictions. The reason for which is that the temperature in this region is lower than that in the middle of the element, so the resistantivity in the middle is greater.
Fig. 5 and Fig. 6 prove that the larger the prospective current, the smaller the time when the ratio of the heat resistance to the cold resistance begins to increase extremely. In other words, the prearcing time is smaller for a larger prospective current. The similar cases exist in the variation of the pre-arcing voltage shown in Fig. 7 and Fig.8. In the breaking tests of low overload currents several changes of pre-arcing voltage are observed by the indicator, before elements melt. There are three times of the voltage increase, this is a indirect evidence of the calculation results. I^2t-I_p characteristic of the single element is given in Fig. 9. While $I_p > 3000A$, the value of I^2t is kept constant, nearly having nothing to do with I_p, when $I_p < 1000A$, the value of I^2t increases rapidly as the prospective current I_p decreases, at the neighbour of 180A, as I_p decreases the value increases slowly, as I_p approaches $1.25I_n$, the value increases rapidly too. It is considered that M-effect has great influence in the range of $1.25I_n$ to 180A, when I_p has the lowest value, which is near the MFC, therefore I^2t has a large value, the heat conduction of element is in action from 200A to 2000A, however, for the large prospective current ($I_p > 3000A$), the adiabatic process is under control.
The comparasion has been made in Fig. 10 between the theoretical curve and tested results. It proves that the deviation between the two is small and the calculation results are helpful for future test.

8. CONCLUSION

The method above may be used to simulate the pre-arcing phenomena of the fuse-element and the acceptable accuracy is achieved in calculation and good correlation is obtained between calculated and measured values of cold resistances and t-I characteristics. Therefore the method could be used in CAD of fuses.

LIST OF PRINCIPAL SYMBOLS

K_x, K_y, K conduction coefficient;
K_t damped coefficient;
ϕ potential function;
$\dot{\phi}$ derivative of potential function;
Ω calculation region;
N_i shape function;
γ electric conductivity;
E electric field strength;
J current density;
IE division number;
ρ mass density, resistantivity;
C thermal capacity, specific heat;
μ surfacial heat discipated coefficient;
C_e f.e.m. division coefficient;
η heat discipated coefficient from the specified elements to tags and end caps.

APPENDIX

PHYSICAL DATA FOR COPPER

ρ_0 resistantivity at the room temperature 1.6961×10^{-6} Ω.cm;
ρ_{01} resistantivity in liquid phase at melting point 21.3×10^{-6} Ω.cm;
α resistance temperature coefficient 0.0045 $^{o}C^{-1}$;
T_m melting point 1084.5 ^{o}C;
H_m melting latent heat 211.4 $J.g^{-1}$;
T_a vaporization temperature 2543 ^{o}C
H_A vaporization latent heat 4752.16 $J.g^{-1}$
K thermal conductivity 4.01 $w.cm^{-1}.^{o}C^{-1}$;
γ density 8.93 $g.cm^{-3}$;
C_{ps} specific heat in solid state 0.385 $w.s.g^{-1}.^{o}C^{-1}$.

PHYSICAL DATA FOR M-SPOTS

T_{sold} melting point 227-231.9 ^{o}C ;
H_s melting latent heat 60.66 $J.g^{-1}$.

OTHER DATA

$K_o = 0.9$, $\tau = 1089$, $I_c = 73A$, $D = 10^{-4}$-10^{-6} $cm^2.s^{-1}$.

REFERENCES

(1) J. G. Leach, P. G. Newbery and A. Wright: "Analysis of high-rupturing-capa bility fuse-link pre-arcing phenomena by a finite-difference method". Proc. IEE, pp987, 1973
(2) Dhatt Canada, Touzot France: "The finite element method displayed". /a book/, 1984
(3) Meng Xianzhong: "Research on low voltage full-range fuse and its pre-arcing characteristics". Master-thesis, Xi'an Jiaotong University, 1986.